

## Effects of initial radius of the interface and Atwood number on nonlinear saturation amplitudes in cylindrical Rayleigh-Taylor instability

Wanhai Liu, Changping Yu, and Xinliang Li

Citation: *Physics of Plasmas* (1994-present) **21**, 112103 (2014); doi: 10.1063/1.4901088

View online: <http://dx.doi.org/10.1063/1.4901088>

View Table of Contents: <http://scitation.aip.org/content/aip/journal/pop/21/11?ver=pdfcov>

Published by the *AIP Publishing*

---

### Articles you may be interested in

[Coupling between interface and velocity perturbations in the weakly nonlinear Rayleigh-Taylor instability](#)

*Phys. Plasmas* **19**, 112706 (2012); 10.1063/1.4766165

[Nonlinear saturation amplitudes in classical Rayleigh-Taylor instability at arbitrary Atwood numbers](#)

*Phys. Plasmas* **19**, 042705 (2012); 10.1063/1.3702063

[Density gradient effects in weakly nonlinear ablative Rayleigh-Taylor instability](#)

*Phys. Plasmas* **19**, 012706 (2012); 10.1063/1.3677821


[Interface width effect on the classical Rayleigh-Taylor instability in the weakly nonlinear regime](#)


*Phys. Plasmas* **17**, 052305 (2010); 10.1063/1.3396369

[Effect of compressibility on the Rayleigh-Taylor and Richtmyer-Meshkov instability induced nonlinear structure at two fluid interface](#)


*Phys. Plasmas* **16**, 032303 (2009); 10.1063/1.3074789

---

A collection of five pieces of Pfeiffer Vacuum equipment, including a red turbopump, a silver turbopump, a silver backing pump, a red turbopump with a long shaft, and a silver chamber component.

 Vacuum Solutions from a Single Source

- Turbopumps
- Backing pumps
- Leak detectors
- Measurement and analysis equipment
- Chambers and components

**PFEIFFER**  **VACUUM**

## Effects of initial radius of the interface and Atwood number on nonlinear saturation amplitudes in cylindrical Rayleigh-Taylor instability

Wanhai Liu,<sup>1,2</sup> Changping Yu,<sup>2</sup> and Xinliang Li<sup>2,a)</sup>

<sup>1</sup>Research Center of Computational Physics, Mianyang Normal University, Mianyang, 621000, China

<sup>2</sup>LHD, Institute of Mechanics, Chinese Academy of Sciences, Beijing 100190, China

(Received 29 September 2014; accepted 24 October 2014; published online 6 November 2014)

Nonlinear saturation amplitudes (NSAs) of the first two harmonics in classical Rayleigh-Taylor instability (RTI) in cylindrical geometry for arbitrary Atwood numbers have been analytically investigated considering nonlinear corrections up to the fourth-order. The NSA of the fundamental mode is defined as the linear (purely exponential) growth amplitude of the fundamental mode at the saturation time when the growth of the fundamental mode (first harmonic) is reduced by 10% in comparison to its corresponding linear growth, and the NSA of the second harmonic can be obtained in the same way. The analytic results indicate that the effects of the initial radius of the interface ( $r_0$ ) and the Atwood number ( $A$ ) play an important role in the NSAs of the first two harmonics in cylindrical RTI. On the one hand, the NSA of the fundamental mode first increases slightly and then decreases quickly with increasing  $A$ . For given  $A$ , the smaller the  $r_0/\lambda$  (with  $\lambda$  perturbation wavelength) is, the larger the NSA of the fundamental mode is. When  $r_0/\lambda$  is large enough ( $r_0 \gg \lambda$ ), the NSA of the fundamental mode is reduced to the prediction of previous literatures within the framework of third-order perturbation theory [J. W. Jacobs and I. Catton, *J. Fluid Mech.* **187**, 329 (1988); S. W. Haan, *Phys. Fluids B* **3**, 2349 (1991)]. On the other hand, the NSA of the second harmonic first decreases quickly with increasing  $A$ , reaching a minimum, and then increases slowly. Furthermore, the  $r_0$  can reduce the NSA of the second harmonic for arbitrary  $A$  at  $r_0 \leq 2\lambda$  while increase it for  $A \leq 0.6$  at  $r_0 \geq 2\lambda$ . Thus, it should be included in applications where the NSA has a role, such as inertial confinement fusion ignition target design. © 2014 AIP Publishing LLC.

[<http://dx.doi.org/10.1063/1.4901088>]

### I. INTRODUCTION

When a fluid supports another fluid of higher density in a gravity field or accelerates another fluid of higher density, the interface between the two fluids will be closely related to Rayleigh-Taylor instability (RTI).<sup>1,2</sup> Assuming a heavier fluid is superposed over a lighter one in a gravitational field  $-g\mathbf{e}_y$ , where  $g$  is acceleration, an initial single-mode cosine modulation, with wave number  $k = 2\pi/\lambda$ , where  $\lambda$  is the perturbation wavelength and small perturbation amplitude  $\varepsilon$  [i.e., the initial perturbation is in the form  $\eta(x, t=0) = \varepsilon \cos(kx)$  with  $k\varepsilon \ll 1$ ] on an interface between two fluids of densities  $\rho_h$  and  $\rho_l$ , is a simplest case. According to the classical linear theory,<sup>1,2</sup> the initial cosine modulation with small amplitude grows exponentially in time  $t$ ,  $\eta_L = \varepsilon e^{\gamma t}$ , where  $\gamma = \sqrt{Ak g}$  is the linear growth rate with  $A = (\rho_h - \rho_l)/(\rho_h + \rho_l)$  being the Atwood number. When the typical perturbation amplitude and its wavelength are of the same order of magnitude, the second and third harmonics are generated successively, and then the perturbation enters the nonlinear regime. Before a strong nonlinear growth regime,<sup>3-6</sup> one has a weakly nonlinear growth regime.<sup>7-17,19-24</sup> Within the framework of the third-order weakly nonlinear theory,<sup>7-11</sup> the interface position at time  $t$  takes the form,  $\eta(x, t) = \eta_1 \cos(kx) + \eta_2 \cos(2kx) + \eta_3 \cos(3kx)$ , where  $\eta_1$ ,  $\eta_2$ , and  $\eta_3$

are, respectively, the amplitudes of the fundamental mode, the second harmonic, and the third harmonic

$$\eta_1 = \eta_L - \frac{1}{16}(3A^2 + 1)k^2\eta_L^3, \quad (1a)$$

$$\eta_2 = -\frac{1}{2}Ak\eta_L^2, \quad (1b)$$

$$\eta_3 = \frac{1}{2}\left(A^2 - \frac{1}{4}\right)k^2\eta_L^3. \quad (1c)$$

It is worth noting that the amplitudes of the second and the third harmonics can be negative. Here, the negative amplitude means the corresponding phase being opposite to the initial cosine modulation's (anti-phase). For problems with large Atwood number,  $A \rightarrow 1$ , Eqs. (1a)–(1c) are reduced to

$$\eta_1 = \eta_L - \frac{1}{4}k^2\eta_L^3, \quad (2a)$$

$$\eta_2 = -\frac{1}{2}k\eta_L^2, \quad (2b)$$

$$\eta_3 = \frac{3}{8}k^2\eta_L^3. \quad (2c)$$

As can be seen in Eq. (1a) or (2a), at the third-order, the growth of the fundamental mode is reduced by the nonlinear mode-coupling effects, i.e., third-order negative feedback to the fundamental mode. According to the previous definition,<sup>8,9,11,23</sup> the transition into the nonlinear regime to occur when the

<sup>a)</sup>Author to whom correspondence should be addressed. Electronic mail: lixl@imech.ac.cn

growth of the fundamental mode is reduced by 10% in comparison to its corresponding linear growth (i.e.,  $\varepsilon e^{\eta t}$ ), we have

$$\frac{\eta_{1s}}{\lambda} = \frac{\sqrt{2}}{\pi\sqrt{5(3A^2 + 1)}}, \tag{3}$$

where  $\eta_{1s}$  is the nonlinear saturation amplitude (NSA) of the fundamental mode with corrections up to the third-order. Let  $A = 1$ , then  $\eta_{1s} \approx 0.1\lambda$  is recovered, which is a typical threshold for nonlinearity widely used.

As mentioned above, the weakly nonlinear behaviors of the RTI in the Cartesian geometry have been a field of theoretical,<sup>7–18</sup> experimental,<sup>19–21</sup> or numerical<sup>22–27</sup> interest. In many applications, the RTI occurs in spherical or cylindrical geometry where the corresponding investigation has been undertaken by several authors;<sup>28–36</sup> specifically, an extra instability due to the curvature of the interface (i.e., the Bell-Plesset effect), the nonlinear evolution of the interface, and numerical solutions including magnetic effects have been addressed. The RTI has a significant role in astrophysics<sup>37–41</sup> and inertial confinement fusion (ICF).<sup>42–53</sup> In astrophysics, the RTI plays a central role in evolutions of many astrophysical phenomena, such as supernova explosion.<sup>39,40</sup> In ICF, at the initial acceleration stage, when the imploding spherical shell is accelerated inward by the low density blow-off plasma, the ablation front is subject to the RTI, and at the later stage, when the compressed fuel starts to decelerate the imploding pusher, the hot spot/shell surface is also prone to the RTI. The RTI can limit the implosion velocity and, in some cases, even break up the implosion shell, resulting in the auto-ignition failure. The ICF targets must be designed to keep the RTI growth at an acceptable level. Therefore, it is central to investigate the NSA of the spherical or cylindrical RTI to better understand and estimate the evolution of the RTI because of its significance in both fundamental research and engineering applications. In this research, NSAs of the first two harmonics in the cylindrical RTI for irrotational, incompressible, and inviscid fluids with a discontinuous profile at arbitrary Atwood numbers are investigated analytically by taking corrections up to the fourth-order into account.

## II. THEORETICAL FRAMEWORK AND EXPLICIT RESULTS

This section is devoted to the detailed description of the theoretical framework of the present paper, and the analytic expressions of amplitudes of the first four harmonics with corrections up to the fourth-order are demonstrated.

A cylindrical coordinate system where  $r$  and  $\theta$  are, respectively, normal and along to the undisturbed interface  $r = \tilde{r}_0$  between two fluids is established. The disturbed interface is located at  $r = a(\theta, t)$  which is always above zero. In the following discussion, we shall denote the properties of the fluid outside the interface by the subscript  $h$  and that inside the interface by the subscript  $l$  unless otherwise stated. Assuming the two fluids in a gravitational field  $-ge_r$  to be irrotational, incompressible, and inviscid, the governing equations for this system are

$$\frac{\partial}{\partial r} \left( r \frac{\partial \phi_i}{\partial r} \right) + \frac{\partial}{\partial \theta} \left( \frac{1}{r} \frac{\partial \phi_i}{\partial \theta} \right) = 0, \quad \text{in two fluids;} \tag{4a}$$

$$\frac{\partial a}{\partial t} + \frac{1}{r^2} \frac{\partial a}{\partial \theta} \frac{\partial \phi_l}{\partial \theta} - \frac{\partial \phi_l}{\partial r} = 0, \quad \text{at } r = a(\theta, t); \tag{4b}$$

$$\frac{\partial a}{\partial t} + \frac{1}{r^2} \frac{\partial a}{\partial \theta} \frac{\partial \phi_h}{\partial \theta} - \frac{\partial \phi_h}{\partial r} = 0, \quad \text{at } r = a(\theta, t); \tag{4c}$$

$$\begin{aligned} & \rho_l \left[ \frac{\partial \phi_l}{\partial t} + \frac{1}{2} \left( \frac{\partial \phi_l}{\partial r} \right)^2 + \frac{1}{2r^2} \left( \frac{\partial \phi_l}{\partial \theta} \right)^2 + gr \right] \\ & - \rho_h \left[ \frac{\partial \phi_h}{\partial t} + \frac{1}{2} \left( \frac{\partial \phi_h}{\partial r} \right)^2 + \frac{1}{2r^2} \left( \frac{\partial \phi_h}{\partial \theta} \right)^2 + gr \right] \\ & + f(t) = 0 \quad \text{at } r = a(\theta, t), \end{aligned} \tag{4d}$$

where  $\phi_i(r, \theta, t)$  are velocity potentials for the two fluids with  $i$  denoting  $h$  or  $l$ , and the interface perturbation  $a(\theta, t)$  corresponds to  $\eta(x, t)$  in Cartesian geometry. The Laplace equation (4a) comes from the incompressibility condition in cylindrical geometry. Equations (4b) and (4c) represent the kinematic boundary conditions in cylindrical geometry (i.e., the normal velocity continuous condition at the interface) that a fluid particle initially situated at the material interface remains at the interface afterwards. The Bernoulli equation (4d) represents the dynamic boundary condition in which the pressure continues across the material interface.

We consider an initial perturbation in the form  $r = a(\theta, t = 0) = r_0 + \varepsilon \cos(\kappa\theta)$ , where  $r_0$  is a positive constant, mode number  $\kappa = 2\pi r_0/\lambda$  and  $\varepsilon \ll \lambda$ . According to principle of mass conservation of the fluid inside the cylindrical interface, i.e.,  $\rho_l \pi \tilde{r}_0^2 = \rho_l \int_{\theta=0}^{2\pi} \int_{r=0}^{r_0 + \varepsilon \cos(\kappa\theta)} r dr d\theta$  where the symbol  $\tilde{r}_0$  is the time-independent average radius of the interface, we especially modify the initial position  $r_0$  as

$$r_0 = \sqrt{\tilde{r}_0^2 - \frac{\varepsilon^2}{2}}. \tag{5}$$

It is obvious that  $r_0 \leq \tilde{r}_0$  with  $\varepsilon$ , specially  $r_0 = \tilde{r}_0$  when  $\varepsilon = 0$ . Due to this small amplitude perturbation in the cylindrical interface, this perturbed interface is prone to RTI. Higher harmonics (i.e., the second harmonic, the third harmonic, and so on) will subsequently be generated by the nonlinear mode-coupling process. Hence, the  $a(\theta, t)$  and  $\phi_i(r, \theta, t)$  can be expanded into a power series in  $\varepsilon$  as

$$\begin{aligned} a(\theta, t) &= \zeta(t)r_0 + \sum_{n=1}^N a^{(n)}(\theta, t) = r_0 \left( 1 + \sum_{n=1}^{\lfloor \frac{N}{2} \rfloor} \varepsilon^{2n} e^{2n\beta t} \alpha_{2n,0} \right) \\ &+ \sum_{n=1}^N \varepsilon^n e^{n\beta t} \sum_{m=0}^{\lfloor \frac{n}{2} \rfloor - 1} \alpha_{n,n-2m} \cos(n-2m)\kappa\theta + O(\varepsilon^{N+1}), \end{aligned} \tag{6a}$$

$$\begin{aligned} \phi_l(r, \theta, t) &= \sum_{n=1}^N \phi_l^{(n)}(r, \theta, t) = \sum_{n=1}^N \varepsilon^n e^{n\beta t} \sum_{m=0}^{\lfloor \frac{n}{2} \rfloor} \phi_{l,n,n-2m} r^{(n-2m)\kappa} \\ &\times \cos(n-2m)\kappa\theta + O(\varepsilon^{N+1}), \end{aligned} \tag{6b}$$

$$\phi_h(r, \theta, t) = \sum_{n=1}^N \phi_h^{(n)}(r, \theta, t) = \sum_{n=1}^N \varepsilon^n e^{n\beta t} \sum_{m=0}^{\lfloor \frac{n}{2} \rfloor} \alpha_{h,n,n-2m} r^{-(n-2m)\kappa} \times \cos(n-2m)\kappa\theta + O(\varepsilon^{N+1}), \tag{6c}$$

where the function  $\zeta(t)$  determines whether the unperturbed interface moves with time: the interface will keep resting when  $\zeta(t) \equiv 1$ ; otherwise, it will move from the initial position  $r(t=0) = r_0$ . The functions  $a^{(n)}(\theta, t)$  and  $\phi_l^{(n)}(r, \theta, t)$  [ $\phi_h^{(n)}(r, \theta, t)$ ] are, respectively,  $n$ th-order perturbed interface and  $n$ th-order perturbed velocity potential for the inner [outer] fluid of the interface when the first four harmonics are taken into account. Regarding the  $(n-2m)$ th Fourier harmonic at the  $n$ th-order, when  $m=0$ ,  $a_{n-2m}^{(n)} = \varepsilon^n e^{n\beta t} \alpha_{n,n-2m}$  [ $\phi_{l,n-2m}^{(n)} = \varepsilon^n e^{n\beta t} \phi_{l,n,n-2m} r^{-(n-2m)\kappa}$  or  $\phi_{h,n-2m}^{(n)} = \varepsilon^n e^{n\beta t} \phi_{h,n,n-2m} r^{-(n-2m)\kappa}$ ] is a generation coefficient of the perturbation interface [generation coefficient of the velocity potential for the light or heavy fluid]; while when  $m > 0$ , it is a correction coefficient of the  $n$ th-order for the perturbation interface [a correction coefficient of the velocity potential for the inner fluid or outer fluid of the interface]. Here, Gauss's symbol  $\lfloor n/2 \rfloor$  denotes the maximum integer that is less than or equal to  $n/2$  and  $\beta$  is the linear growth rate in the cylindrical geometry. Note that the perturbation velocity potentials  $\phi_h(r, \theta, t)$  and  $\phi_l(r, \theta, t)$  have satisfied the Laplace equation (4a) and the boundary conditions  $\nabla\phi_h|_{r \rightarrow +\infty} = 0$  and  $\nabla\phi_l|_{r=0} = 0$ . And  $\alpha_{1,1} = 1$  when the initial condition is taken into account. The coupling factors in the amplitudes of the Fourier harmonic,  $\alpha_{n,n-2m}$ , ( $n = 2, \dots, N$ , and  $m = 0, 1, \dots, \lfloor n/2 \rfloor$ ) and  $\beta$  are what we ultimately intend to determine.

It should be emphasized that the procedure of the solving this system is a key point. The detailed steps are

- (i) Substituting Eqs. (6a)–(6c), in which  $O(\varepsilon^{N+1})$  is neglected, into Eqs. (4b)–(4d).
- (ii) Replacing  $r$  in these three equations with Eq. (6a).
- (iii) Reexpressing the left hand sides of the resulting equations into Maclaurin series of  $\varepsilon$  and collecting terms of the same power in  $\varepsilon$  to construct a set of equations.
- (iv) Eliminating unknown factors in the velocity potentials and solving the resulting equations successively for  $n = 1, 2, \dots, N$ .

Comparing the procedures applied into the similar problems in Cartesian geometry, steps (i)–(iii) are somewhat different. In Cartesian geometry, the initially unperturbed interface keeps invariable with the development of the RTI, and hence, the formal method is to expand all the physical quantities on this initial interface. Thus, one obtains the equations holding on the initial interface, instead of those constructing on the developing interface. In view of the initial unperturbed interface moving with the development of the perturbation, we do not use the formal approach in this research. It is interesting that we have, respectively, performed these two different methods and obtained the same results. However, the method provided here is confirmed to be much simpler than the formal one by the calculations at the same conditions.

The linear growth rate and coupling factors of the first four harmonics with corrections up to the fourth-order [i.e.,  $N = 4$  in Eqs. (6a)–(6c)] can be expressed as

$$\beta = \sqrt{\frac{Ag\kappa}{r_0}}, \tag{7a}$$

$$\alpha_{2,0} = -\frac{1}{4r_0^2}, \tag{7b}$$

$$\alpha_{2,2} = -\frac{A\kappa + 1}{2r_0}, \tag{7c}$$

$$\alpha_{3,1} = \frac{-3A^2\kappa^2 + A\kappa - \kappa^2 + 9}{16r_0^2}, \tag{7d}$$

$$\alpha_{3,3} = \frac{4A^2\kappa^2 + 7A\kappa - \kappa^2 + 3}{8r_0^2}, \tag{7e}$$

$$\alpha_{4,0} = \frac{A^2\kappa^2 - 5A\kappa + \kappa^2 - 12}{32r_0^4}, \tag{7f}$$

$$\alpha_{4,2} = \frac{123A^3\kappa^3 + 135A^2\kappa^2 + A(11\kappa^2 - 173)\kappa + 78\kappa^2 - 228}{336r_0^3}, \tag{7g}$$

$$\alpha_{4,4} = -\frac{16A^3\kappa^3 + 39A^2\kappa^2 - 8A\kappa^3 + 31A\kappa - 9\kappa^2 + 8}{24r_0^3}. \tag{7h}$$

Expression (7a) shows that the linear growth rates in Cartesian and cylindrical geometries are different unless  $\kappa/r_0 = k$  (i.e., the same  $\lambda$ ). Keeping Atwood number  $A$ , acceleration  $g$ , and mode number  $\kappa$  invariable, the smaller the initial radius of the interface  $r_0$  is, the larger the linear growth rate in the cylindrical geometry is. Expression (7c) denotes that the second harmonic has a character of negative growth (i.e., anti-phase). In addition, expressions (7c)–(7h) demonstrate that coupling factors are influenced by not only  $A$  but also  $\kappa$  and  $r_0$ . If the constant  $\lambda$  is considered in both the cylindrical and Cartesian geometries [i.e.,  $\kappa/r_0 = k$ ], and  $r_0$  is large [i.e.,  $r_0 \rightarrow +\infty$ ],  $\alpha_{n,n-2m}/k^{n-1}$  ( $n = 2, \dots, N$ , and  $m = 0, 1, \dots, \lfloor n/2 \rfloor$ ) will be simplified to the corresponding Atwood number  $f_{n,n-2m}$  in work.<sup>11</sup> This means that under the conditions of the same  $\lambda$  and large  $r_0$ , the perturbed interface in cylindrical geometry will reproduce that in Cartesian geometry, and the results from the classical third-order weakly nonlinear theory,<sup>7–11</sup> as shown in Eqs. (1a)–(1c), are recovered. It should be noted that the generation of  $\alpha_{2,0}$  and  $\alpha_{4,0}$  is an essential character different from the results in Cartesian geometry where  $\alpha_{2,0} = \alpha_{4,0} = 0$ .

Accordingly, the interface position at the framework of the fourth-order theory in the cylindrical geometry takes the form  $\zeta r_0 + a(\theta, t) \doteq \zeta r_0 + \sum_{n=1}^4 a_n \cos(n\kappa\theta)$ , where  $\zeta$  and the amplitude of the  $n$ th harmonic,  $a_n$ , are

$$\zeta = 1 + \eta_{Lc}^2 (\alpha_{2,0} + \alpha_{4,0} \eta_{Lc}^2), \tag{8a}$$

$$a_1 = \eta_{Lc} (1 + \alpha_{3,1} \eta_{Lc}^2), \tag{8b}$$

$$a_2 = \eta_{Lc}^2 (\alpha_{2,2} + \alpha_{4,2} \eta_{Lc}^2), \tag{8c}$$



$$a_3 = \alpha_{3,3}\eta_{Lc}^3, \tag{8d}$$

$$a_4 = \alpha_{4,4}\eta_{Lc}^4, \tag{8e}$$

where  $\eta_{Lc} = \varepsilon e^{\beta t}$  is the linear growth amplitude of the fundamental mode in the cylindrical geometry. It should be pointed out that the amplitudes of the first two harmonics are corrected by the higher harmonics (the third and the fourth harmonics), but the third and the fourth harmonics are not, to this order of approximation. As stated just now, an essential character different from the Cartesian RTI is that the zeroth harmonic does not vanish in cylindrical RTI [see Eq. (8a)]. This means that the position of the initial unperturbed interface  $r = r_0$  will be changed into  $r = \zeta(t)r_0$  with the development of the perturbation, differing entirely from that in Cartesian space where the initial unperturbed interface keeps invariable all the time.

### III. NSA OF THE FUNDAMENTAL MODE

Considering the third-order (fourth-order) nonlinear correction to the fundamental mode (second harmonic), the NSA of the fundamental mode (second harmonic) can be determined. In this section and Sec. IV, we shall analyze the NSAs of the fundamental mode and the second harmonic, respectively, with corrections up to the fourth-order.

As mentioned above, the NSA of the fundamental mode can be defined as the linear growth amplitude of the fundamental mode ( $\sim e^{\beta t}$ ) at the saturation time ( $t_{1s}$ ) when the growth of the fundamental mode is reduced by 10% in comparison to its corresponding linear growth. Hence, we have

$$\frac{\varepsilon e^{\beta t_{1s}} - a_1(t_{1s})}{\varepsilon e^{\beta t_{1s}}} = \frac{1}{10}. \tag{9}$$

Here,  $\beta$  and  $a_1$  are, respectively, substituted by Eqs. (7a) and (8b), and the saturation time  $t_{1s}$  of the fundamental mode can be obtained by solving the resulting equation (9). It is

$$t_{1s} = \sqrt{\frac{r_0}{Ag\kappa}} \log \left( \frac{2r_0}{\varepsilon} \frac{\sqrt{\frac{2}{5}}}{\sqrt{3A^2\kappa^2 - A\kappa + \kappa^2 - 9}} \right). \tag{10}$$

Then, the NSA of the fundamental mode with corrections up to the third-order is determined as  $a_{1s} = \eta_{Lc}(t_{1s}) = \varepsilon e^{\beta t_{1s}}$ , i.e.,

$$a_{1s} = 2\sqrt{\frac{2}{5}} \sqrt{\frac{r_0^2}{3A^2\kappa^2 - A\kappa + \kappa^2 - 9}}. \tag{11}$$

Using mode number  $\kappa = 2\pi r_0/\lambda$ , the normalized saturation time and NSA of the fundamental mode are

$$\frac{t_{1s}}{\sqrt{\lambda/g}} = \frac{1}{\sqrt{2A\pi}} \log 2 \sqrt{\frac{2r_0^2}{5\varepsilon(12\pi^2 A^2 r_0^2 - 2\pi A r_0 + 4\pi^2 r_0^2 - 9)}}, \tag{12a}$$

$$\frac{a_{1s}}{\lambda} = \frac{2\sqrt{2}r_0}{\sqrt{5}\sqrt{12\pi^2 A^2 r_0^2 - 2\pi A r_0 + 4\pi^2 r_0^2 - 9}}, \tag{12b}$$

respectively. When the limit of  $r_0 \rightarrow +\infty$  is taken into account, we have

$$\frac{t_{1s}^\infty}{\sqrt{\lambda/g}} = \frac{1}{\sqrt{2A\pi}} \log \sqrt{\frac{2}{5\varepsilon\pi^2(3A^2 + 1)}}, \tag{13a}$$

$$\frac{a_{1s}^\infty}{\lambda} = \frac{\sqrt{2}}{\pi\sqrt{5}\sqrt{3A^2 + 1}}. \tag{13b}$$

As can be seen, when  $r_0/\lambda$  is large enough (i.e.,  $r_0/\lambda \rightarrow +\infty$ ), NSA of the fundamental mode in the cylindrical geometry will tend to that in the Cartesian geometry, i.e., Eq. (3) is recovered. This means the cylindrical effect on NSA of the fundamental mode will vanish.

We show the normalized saturation time,  $(g/\lambda)^{1/2}t_{1s}$ , and the normalized NSA,  $a_{1s}/\lambda$ , of the fundamental mode with different Atwood number  $A$  and the initial radius of the interface  $r_0$  in Figures 1 and 2. Here,  $r_0/\lambda = 0.6, 0.7, 0.8, 0.9, 1.0, 1.5, 2.0$ , and  $+\infty$  are uniformly selected.

Figure 1 shows that the normalized saturation time of the fundamental mode first drops swiftly and then decreases tardily with  $A$ . For fixed  $A$ , the normalized saturation time of the fundamental mode increases with the decreasing  $r_0/\lambda$ . This means that with the decreasing  $A$  or  $r_0/\lambda$ , the time spent on the linear growth of the fundamental mode becomes long, especially for the small  $A$  ( $A \leq 0.1$ ).

Figure 2 demonstrates that the normalized NSA of the fundamental mode decreases monotonously with  $A$  for large  $r_0$  (corresponding to the Cartesian geometry), while it first increases weakly to a peak and then decreases strongly with  $A$  for finite  $r_0/\lambda$ . Thus, there will appear a critical  $A_{c1}$ . For  $A \leq A_{c1}$ , the NSA keeps increasing to a maximum with  $A$ ; otherwise, it keeps decreasing with  $A$ . Meanwhile, the  $A_{c1}$  has a trend of increasing with decreasing  $r_0/\lambda$ . For a selected  $A$ , the NSA of the fundamental mode increases with the decreasing  $r_0/\lambda$ . It appears evident that  $r_0$  has a significant influence on NSA of the fundamental mode particularly when  $r_0 < \lambda$ . As can be seen, the normalized NSA of the fundamental mode at  $A = 1$  and  $r_0/\lambda = 0.6$  is 0.114, while

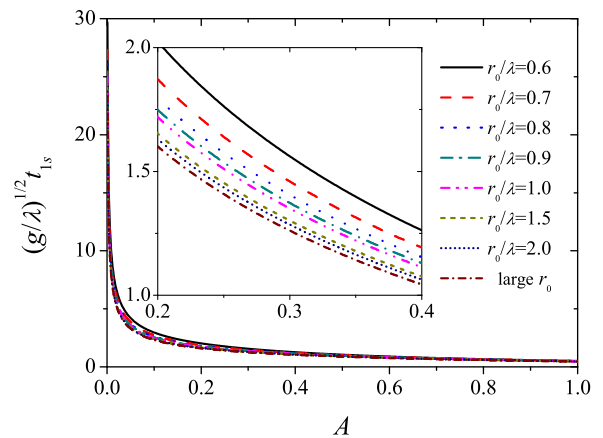


FIG. 1. The normalized saturation time of the fundamental mode,  $(g/\lambda)^{1/2}t_{1s}$ , versus arbitrary  $A$  for different initial radius of the cylindrical interface. The result of large  $r_0$  corresponds to that of the Cartesian geometry. The initial perturbation amplitude of the interface is fixed as  $\varepsilon/\lambda = 0.001$ . The insert is a local graph.

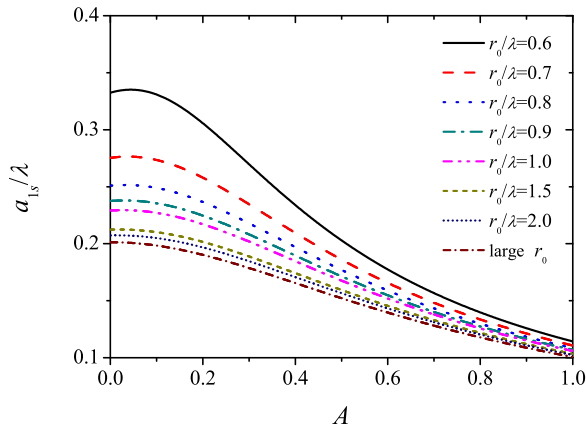


FIG. 2. The normalized NSA of the fundamental mode,  $a_{1s}/\lambda$ , versus arbitrary  $A$  for different initial radius of the cylindrical interface. The result of large  $r_0$  corresponds to that of the Cartesian geometry.

that at  $A = 1$  for large  $r_0$  is only 0.1. Furthermore, at  $A = 0$  and  $r_0/\lambda = 0.6$ , the NSA of the fundamental mode is 0.333, while the corresponding result in the Cartesian geometry is just 0.201. Accordingly, the cylindrical effects (especially small  $r_0/\lambda$ ) play an important role in the NSA of the fundamental mode for arbitrary  $A$ .

Note that Figure 2 merely shows the NSA of the fundamental mode for  $\kappa \geq 4$ . For the  $\kappa < 4$  configuration, the NSA of the fundamental mode cannot entirely be predicted by the weakly nonlinear analysis up to the fourth-order. From the NSA definition of the fundamental mode, it is the negative feedback (reduction effect) to the growth of the fundamental mode that results in the occurrence of the NAS of the fundamental mode. For the fundamental mode, just the third harmonic provides a feedback that is either a positive one when  $\alpha_{3,1} > 0$  or a negative one when  $\alpha_{3,1} < 0$ . The  $\alpha_{3,1}$  for  $\kappa$  from 1 to 3 versus variable  $A$  is shown in Figure 3. It is clear that  $\alpha_{3,1}$  is above zero at  $\kappa = 1$  for arbitrary  $A$ , and  $\alpha_{3,1}$  is less than zero only when either both  $\kappa = 2$  and  $A \geq 0.74$  or both  $\kappa = 3$  and  $A \geq 0.11$ . Accordingly, when the weakly nonlinear analysis is performed just up to fourth-order, the correction to the fundamental mode from the third harmonic is

not always a negative feedback for different  $\kappa$  and  $A$ , which generates failure of the NSA of the fundamental mode for some configurations.

For the further insight into the NSA of the fundamental mode, we forward the perturbation analysis up to the fifth-order, among which the fifth-order results related to the interface are given in the Appendix, and mode coupling factor  $\alpha_{5,1}$  is shown in Figure 4. Figure 4 reads that although  $\alpha_{5,1} > 0$  at  $\kappa = 1$  for arbitrary  $A$ , the positive or negative sign of  $\alpha_{5,1}$  at  $\kappa = 2$  and 3 changes with  $A$ . For  $\kappa = 2$ ,  $\alpha_{5,1} < 0$  when  $A \leq 0.04$ ; whereas for  $\kappa = 3$ ,  $\alpha_{5,1} < 0$  when  $A \leq 0.4$ . Thus, with the order of the corrections increasing, the negative feedbacks to the fundamental mode will cover the whole space of the parameters including  $\kappa$  and  $A$ . Furthermore, the later the first negative feedback stemming from the higher-order harmonic appears, the larger the NSA of the fundamental mode is. We, therefore, can predict that for the fixed  $A$ , the NSA of the fundamental mode increases with the decreasing  $\kappa$ , especially for the case of the lower-mode numbers (such as,  $\kappa < 4$  case). In fact, this trend has been denoted in Figure 2.

#### IV. NSA OF THE SECOND HARMONIC

The concept of the NSA of the fundamental mode in Sec. III will be extended for the second harmonic in this section. The NSA of the second harmonic is defined as the linear growth amplitude of the second harmonic ( $\sim e^{2\beta t}$ ) at the saturation time ( $t_{2s}$ ) when the growth of the second harmonic is reduced by 10% in comparison to its corresponding linear growth.

The saturation time  $t_{2s}$  of the second harmonic with corrections up to the fourth-order can be obtained from the following:

$$\frac{\alpha_{2,2}\varepsilon^2 e^{2\beta t_{2s}} - a_2(t_{2s})}{\alpha_{2,2}\varepsilon^2 e^{2\beta t_{2s}}} = \frac{1}{10}. \quad (14)$$

Substituting Eqs. (7a), (8c), (7c), and (7g) to this equation, the saturation time of the second harmonic with the corrections up to the fourth-order can be determined as

$$t_{2s} = \sqrt{\frac{r_0}{Ag\kappa}} \log \sqrt{\frac{84r_0^2(A\kappa + 1)}{5\varepsilon^2(123A^3\kappa^3 + 135A^2\kappa^2 + 11A\kappa^3 - 173A\kappa + 78\kappa^2 - 228)}}. \quad (15)$$

Then, the NSA of the second harmonic with corrections up to the fourth-order is determined as  $a_{2s} = \alpha_{2,2}\eta_{Lc}^2(t_{2s}) = \alpha_{2,2}\varepsilon^2 e^{2\beta t_{2s}}$ , i.e.,

$$a_{2s} = -\frac{42r_0(A\kappa + 1)^2}{5(123A^3\kappa^3 + 135A^2\kappa^2 + 11A\kappa^3 - 173A\kappa + 78\kappa^2 - 228)}. \quad (16)$$

Adopting mode number  $\kappa = 2\pi r_0/\lambda$ , the normalized saturation time and NSA of the second harmonic are

$$\frac{t_{2s}}{\sqrt{\lambda/g}} = \frac{1}{\sqrt{2A\pi}} \log \sqrt{\frac{42r_0^2(2\pi Ar_0 + 1)}{5\varepsilon^2(492\pi^3 A^3 r_0^3 + 270\pi^2 A^2 r_0^2 + 44\pi^3 A r_0^3 - 173\pi A r_0 + 156\pi^2 r_0^2 - 114)}}, \quad (17a)$$

$$\frac{a_{2s}}{\lambda} = -\frac{21r_0(2\pi Ar_0 + 1)^2}{5(492\pi^3 A^3 r_0^3 + 270\pi^2 A^2 r_0^2 + 44\pi^3 A r_0^3 - 173\pi A r_0 + 156\pi^2 r_0^2 - 114)}, \quad (17b)$$

respectively. When taking the limit of  $r_0 \rightarrow +\infty$  into account, we have

$$\frac{t_{2s}^\infty}{\sqrt{\lambda/g}} = \frac{1}{\sqrt{2A\pi}} \log \sqrt{\frac{21}{5\epsilon^2 \pi^2 (123A^2 + 11)}}, \quad (18a)$$

$$\frac{a_{2s}^\infty}{\lambda} = -\frac{21A}{5\pi(123A^2 + 11)}. \quad (18b)$$

As can be seen, when  $r_0/\lambda$  is large enough (i.e.,  $r_0/\lambda \rightarrow +\infty$ ), NSA of the second harmonic in the cylindrical geometry will tend to the corresponding NSA in the Cartesian geometry. This means the cylindrical effect on NSA of the second harmonic to vanish.

The normalized saturation time,  $(g/\lambda)^{1/2}t_{2s}$ , and the normalized NSA,  $a_{2s}/\lambda$ , of the second harmonic with different Atwood number  $A$  and the initial radius  $r_0$  of the interface are shown in Figures 5 and 6. Here,  $r_0/\lambda = 0.6, 0.7, 0.8, 0.9, 1.0, 1.5, 2.0$ , and  $+\infty$  are taken into account in Figure 5 and  $r_0/\lambda = 0.6, 0.7, 0.8, 0.9, 1.0, 1.5, 2.0, 10, 50, 250$ , and  $+\infty$  are considered in Figure 6.

Comparing Figures 5 and 1, one finds that the normalized time  $(g/\lambda)^{1/2}t_{2s}$  of the second harmonic has the same trend with  $A$  or  $r_0$  as that of the fundamental mode. With the

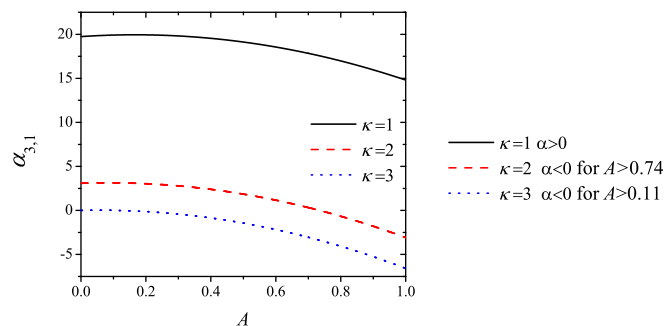


FIG. 3. The coupling factor  $\alpha_{3,1}$  for mode numbers  $\kappa = 1$  (solid line), 2 (dashed line), 3 (dotted line) with different  $A$ .

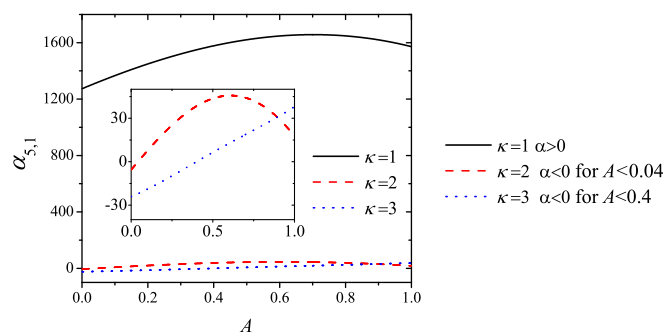


FIG. 4. The coupling factor  $\alpha_{5,1}$  for mode numbers  $\kappa = 1$  (solid line), 2 (dashed line), 3 (dotted line) with different  $A$ . The insert is just the graph concerning  $\kappa = 2$  and 3.

same  $A$  and  $r_0$ , the  $(g/\lambda)^{1/2}t_{2s}$  is constantly larger than  $(g/\lambda)^{1/2}t_{1s}$ . As for the NSA of the second harmonic, it is found from Figure 6 that the NSA first decreases to some value quickly and then increases slowly with  $A$  for arbitrary  $r_0$ . Therefore, there also exists a critical  $A_{c2}$ . When  $A \leq A_{c2}$ , the NSA decreases with  $A$ ; otherwise, it increases with  $A$ . An interesting thing is that the  $A_{c2}$  is related with  $r_0$ . For smaller  $r_0$  ( $r_0 \leq 2.0\lambda$ ), the  $A_{c2}$  keeps a constant (0.4 or so); otherwise, the  $A_{c2}$  abates with the decreasing  $r_0$ . In addition, for smaller  $r_0$  ( $r_0 \leq 2.0\lambda$ ), the  $r_0$  affects NSA for arbitrary  $A$ , while for the larger  $r_0$ , the  $r_0$  has a more distinct influence on NSA for  $A \leq 0.6$  than  $A \geq 0.6$ .

Comparing the NSA of the second harmonic with that of the fundamental mode, one sees that the NSAs of the first two harmonics can be determined with the reductions of the higher-order harmonics. On the one hand, for arbitrary  $A$ , in view of the positive growth of the fundamental mode, the NSA of the fundamental mode stands above zero; while for the negative growth of the second harmonic ( $\alpha_{2,2} < 0$ ), the NSA of the second harmonic is less than zero. On the other hand, with the increasing  $A$ , the absolute values of the NSAs of the first two harmonics increase to some maximum and then decrease. For the NSA of the fundamental mode, the critical  $A_{c1}$ , which corresponds to the maximum value of the NSA of the fundamental mode, tends to zero with the increasing  $r_0/\lambda$ ; whereas for that of the second harmonic, the critical  $A_{c2}$  tends to 0.3 or so with the increasing  $r_0/\lambda$ . Meanwhile, the absolute value of the NSA of the fundamental mode is always larger than that of the second harmonic for the selected  $A$  and  $r_0/\lambda$ .

It should be noted that, for the NSAs of the first two harmonics, the above discussed case that the acceleration is in the form  $-ge_r$  (i.e.,  $g > 0$ ) and the lighter (heavier) fluid locates at insider (outside) the interface can readily be extended to the reversed case where  $g < 0$  and  $A < 0$ . As a result, the results of the NSAs of the first two harmonics

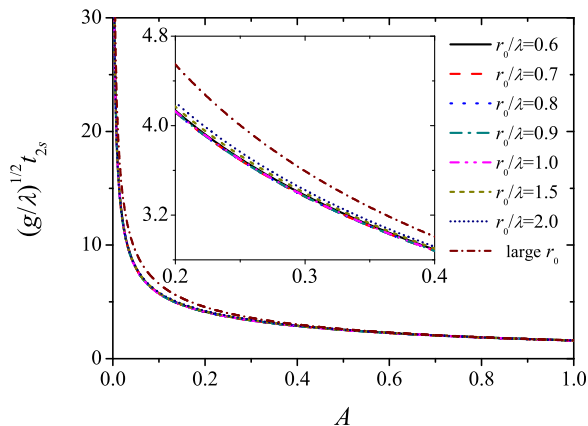


FIG. 5. The normalized saturation time of the second harmonic,  $(g/\lambda)^{1/2}t_{2s}$ , versus arbitrary  $A$  for different initial radius of the cylindrical interface. The result of large  $r_0$  corresponds to that of the Cartesian geometry. The initial perturbation amplitude of the interface is fixed as  $\epsilon/\lambda = 0.001$ . The insert is a local graph.

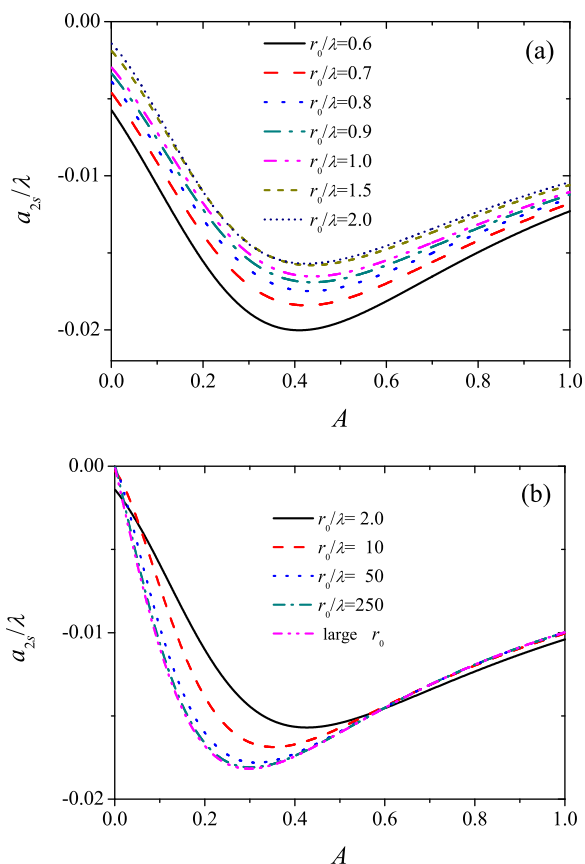


FIG. 6. The normalized NSA of the second harmonic,  $a_{2s}/\lambda$ , versus arbitrary  $A$  for different initial radius of the cylindrical interface. The initial radius  $r_0$  is taken as  $0.6\lambda$ ,  $0.7\lambda$ ,  $0.8\lambda$ ,  $0.9\lambda$ ,  $1.0\lambda$ ,  $1.5\lambda$ , and  $2.0\lambda$  in (a) and  $2.0\lambda$ ,  $10\lambda$ ,  $50\lambda$ , and  $250\lambda$  in (b). The result of large  $r_0$  corresponds to that of the Cartesian geometry.

include those for the case where  $g > 0$  and  $A > 0$ , and those for the latter case where  $g < 0$  and  $A < 0$ .

## V. CONCLUSION

In this investigation, we have analytically explored the NSAs of the first two harmonics in the classical RTI (irrotational, incompressible, and inviscid fluids) with a discontinuous profile in cylindrical geometry for arbitrary Atwood numbers with nonlinear corrections up to the fourth-order. The prediction of the NSA of the fundamental mode with corrections up to the third-order from classical weakly nonlinear theory<sup>7-11</sup> is recovered when the initial radius of the interface normalized by perturbation wavelength tends to infinity.

For the NSA of the fundamental mode in the cylindrical geometry, it has a different variable trend with Atwood number  $A$  from the NSA in the Cartesian geometry. The NSA of the fundamental mode in Cartesian geometry decreases monotonously with increasing  $A$ ; while cylindrical effects taken into account, it first slightly increases to a maximum and then decreases with  $A$ . Accordingly, there will be a critical  $A_{c1}$  which is small. When  $A \leq A_{c1}$ , the NSA keeps increasing generally with  $A$ ; while when  $A > A_{c1}$ , the NSA keeps decreasing quickly with increasing  $A$ . It is also found that the smaller the normalized initial radius of the interface  $r_0/\lambda$  is, the larger the  $A_{c1}$  is. Again, the  $r_0$  plays a vital role in NSA of the fundamental mode. The NSA of the fundamental mode increases with decreasing  $r_0/\lambda$ , especially when  $r_0$  is compared to  $\lambda$ . For the NSA of the second harmonic, it first decreases quickly with increasing  $A$ , reaching a minimum, and then increases slowly, and hence, there is another critical Atwood number  $A_{c2}$ . When  $A \leq A_{c2}$ , the NSA of the second harmonic decreases monotonously with increasing  $A$ ; otherwise, it increases monotonously with increasing  $A$ . The  $A_{c2}$  decreases with decreasing  $r_0/\lambda$ . Furthermore, the  $r_0$  can reduce the NSA of the second harmonic for arbitrary  $A$  at  $r_0 \leq 2\lambda$  while increase it for  $A \leq 0.6$  at  $r_0 \geq 2\lambda$ . Our analytic results show that not only the Atwood number but also the initial radius of the interface strikingly influences the NSA of the RTI. Thus, it should be included in applications where the NSA plays a role, such as inertial confinement fusion ignition target design.

## ACKNOWLEDGMENTS

The author (Liu) would like to thank Professor X. T. He and Professor W. H. Ye for their fruitful discussions. The authors would also like to thank the anonymous referee for the valuable suggestions that greatly improved this paper. This work was supported by the National Natural Science Foundation of China (Grant Nos. 11472278 and 11372330), the Scientific Research Foundation of Mianyang Normal University (Grant Nos. QD2014A009 and 2014A02) and the National High-Tech ICF Committee.

## APPENDIX: COUPLING FACTORS OF THE FIFTH HARMONIC

Mode coupling factors of the fifth-order results related to the perturbation interface are

$$\alpha_{5,1} = \frac{165A^4\kappa^4 - 1044A^3\kappa^3 + A^2(452\kappa^2 - 1907)\kappa^2 + A(110\kappa^2 + 3253)\kappa + 35\kappa^4 - 1742\kappa^2 + 6100}{5376r_0^4},$$

$$\alpha_{5,3} = \frac{-21612A^4\kappa^4 - 42569A^3\kappa^3 + 4239A^2\kappa^4 - 840A^2\kappa^2 - 8718A\kappa^3 + 43772A\kappa + 1008\kappa^4 - 19587\kappa^2 + 24875}{29568r_0^4},$$

$$\alpha_{5,5} = \frac{400A^4\kappa^4 + 1240A^3\kappa^3 - 296A^2\kappa^4 + 1411A^2\kappa^2 - 590A\kappa^3 + 696A\kappa + 21\kappa^4 - 306\kappa^2 + 125}{384r_0^4}.$$



- <sup>1</sup>L. Rayleigh, Proc. London Math. Soc. **14**, 170 (1883).
- <sup>2</sup>G. Taylor, Proc. R. Soc. London, Ser. A **201**, 192 (1950).
- <sup>3</sup>Q. Zhang, Phys. Rev. Lett. **81**(16), 3391 (1998).
- <sup>4</sup>K. O. Mikaelian, Phys. Rev. E **67**, 026319 (2003).
- <sup>5</sup>V. N. Goncharov, Phys. Rev. Lett. **88**(13), 134502 (2002).
- <sup>6</sup>P. Ramaprabhu, G. Dimonte, Y. N. Young, A. C. Calder, and B. Fryxell, Phys. Rev. E **74**, 066308 (2006).
- <sup>7</sup>D. Layzer, Astrophys. J. **122**, 1 (1955).
- <sup>8</sup>J. W. Jacobs and I. Catton, J. Fluid Mech. **187**, 329 (1988).
- <sup>9</sup>S. W. Haan, Phys. Fluids B **3**, 2349 (1991).
- <sup>10</sup>M. Berning and A. M. Rubenchik, Phys. Fluids **10**, 1564 (1998).
- <sup>11</sup>W. H. Liu, L. F. Wang, W. H. Ye, and X. T. He, Phys. Plasmas **19**, 042705 (2012).
- <sup>12</sup>S. Hasegawa and K. Nishihara, Phys. Plasmas **2**(12), 4606 (1995).
- <sup>13</sup>J. Sanz, J. Ramirez, R. Ramis, R. Betti, and R. P. J. Town, Phys. Rev. Lett. **89**, 195002 (2002).
- <sup>14</sup>T. Ikegawa and K. Nishihara, Phys. Rev. Lett. **89**, 115001 (2002).
- <sup>15</sup>J. Garnier and L. Masse, Phys. Plasmas **12**, 062707 (2005).
- <sup>16</sup>S. I. Sohn, Phys. Rev. E **67**, 026301 (2003).
- <sup>17</sup>V. N. Goncharov and D. Li, Phys. Rev. E **71**, 046306 (2005).
- <sup>18</sup>M.-A. Lafay, B. Le Creurer, and S. Gauthier, Europhys. Lett. **79**, 64002 (2007).
- <sup>19</sup>B. A. Remington, S. W. Haan, S. G. Glendinning, J. D. Kilkenny, D. H. Munro, and R. J. Wallace, Phys. Fluids B **4**(4), 967 (1992).
- <sup>20</sup>B. A. Remington, S. V. Weber, M. M. Marinak, S. W. Haan, J. D. Kilkenny, R. J. Wallace, and G. Dimonte, Phys. Plasmas **2**(1), 241 (1995).
- <sup>21</sup>V. A. Smalyuk, V. N. Goncharov, T. R. Boehly, J. P. Knauer, D. D. Meyerhofer, and T. C. Sangster, Phys. Plasmas **11**(11), 5038 (2004).
- <sup>22</sup>M. J. Dunning and S. W. Haan, Phys. Plasmas **2**(5), 1669 (1995).
- <sup>23</sup>L. F. Wang, W. H. Ye, Z. F. Fan, and Y. J. Li, Europhys. Lett. **90**, 15001 (2010).
- <sup>24</sup>L. F. Wang, W. H. Ye, and Y. J. Li, Phys. Plasmas **17**, 052305 (2010).
- <sup>25</sup>C. Mügler and S. Gauthier, Phys. Rev. E **58**, 4548 (1998).
- <sup>26</sup>A. Rikanati, U. Alon, and D. Shvarts, Phys. Rev. E **58**, 7410 (1998).
- <sup>27</sup>L. F. Wang, W. H. Ye, Z. F. Fan, Y. J. Li, X. T. He, and M. Y. Yu, Europhys. Lett. **86**, 15002 (2009).
- <sup>28</sup>Q. Zhang and M. J. Graham, Phys. Fluids **10**, 974 (1998).
- <sup>29</sup>M. A. Sweeney and F. C. Perry, J. Appl. Phys. **52**, 4487 (1981).
- <sup>30</sup>S. T. Weir, E. A. Chandler, and B. T. Goodwin, Phys. Rev. Lett. **80**, 3763 (1998).
- <sup>31</sup>Z. F. Fan, S. P. Zhu, W. B. Pei, W. H. Ye, M. Li, X. W. Xu, J. F. Wu, Z. Z. Dai, and L. F. Wang, Europhys. Lett. **99**, 65003 (2012).
- <sup>32</sup>R. Epstein, Phys. Plasmas **11**, 5114 (2004).
- <sup>33</sup>P. Amendt, Phys. Plasmas **13**, 042702 (2006).
- <sup>34</sup>K. Chambers and L. K. Forbes, Phys. Plasmas **19**, 102111 (2012).
- <sup>35</sup>C. Matsuoka and K. Nishihara, Phys. Rev. E **73**, 026304 (2006).
- <sup>36</sup>W. H. Liu, C. P. Yu, W. H. Ye, L. F. Wang, and X. T. He, Phys. Plasmas **21**, 062119 (2014).
- <sup>37</sup>V. N. Gamezo, A. M. Khokhlov, E. S. Oran, A. Y. Chtchelkanova, and R. O. Rosenburg, Science **299**, 77 (2003).
- <sup>38</sup>B. A. Remington, R. P. Drake, and D. D. Ryutov, Rev. Mod. Phys. **78**, 755 (2006).
- <sup>39</sup>T. Ebisuzaki, T. Shigezumi, and K. Nomoto, Astrophys. J. **344**, L65 (1989).
- <sup>40</sup>I. Hachisu, T. Matsuda, K. Nomoto, and T. Shigezumi, Astrophys. J. **358**, L57 (1990).
- <sup>41</sup>R. P. Drake, High-Energy-Density Physics: Fundamentals, Inertial Fusion and Experimental Astrophysics (Springer, New York, 2006).
- <sup>42</sup>J. Nuckolls, L. Wood, A. Thiessen, and G. Zimmerman, Nature **239**, 139 (1972).
- <sup>43</sup>S. Bodner, Phys. Rev. Lett. **33**, 761 (1974).
- <sup>44</sup>H. Takabe, K. Mima, L. Montierth, and R. L. Morse, Phys. Fluids **28**, 3676 (1985).
- <sup>45</sup>M. Tabak, D. H. Munro, and J. D. Lindl, Phys. Fluids B **2**, 1007 (1990).
- <sup>46</sup>V. N. Goncharov, R. Betti, R. L. McCrory, P. Sorotokin, and C. P. Verdon, Phys. Plasmas **3**(4), 1402 (1996).
- <sup>47</sup>S. G. Glendinning, S. N. Dixit, B. A. Hammel, D. H. Kalantat, M. H. Key, J. D. Kilkenny, J. P. Knauer, D. M. Pennington, B. A. Remington, R. J. Wallace, and S. V. Weber, Phys. Rev. Lett. **78**, 3318 (1997).
- <sup>48</sup>K. Shigemori, H. Azechi, M. Nakai, M. Honda, K. Meguro, N. Miyanaga, H. Takabe, and K. Mima, Phys. Rev. Lett. **78**, 250 (1997).
- <sup>49</sup>A. R. Piriz, Phys. Plasmas **8**(3), 997 (2001).
- <sup>50</sup>W. H. Ye, W. Y. Zhang, and X. T. He, Phys. Rev. E **65**, 057401 (2002).
- <sup>51</sup>S. Atzeni and J. Meyer-ter-Vehn, The Physics of Inertial Fusion: Beam Plasma Interaction Hydrodynamics, Hot Dense Matter (Oxford University, Oxford, 2004).
- <sup>52</sup>J. D. Lindl, P. Amendt, R. L. Berger, S. G. Glendinning, S. H. Glenzer, S. W. Haan, R. L. Kauffman, O. L. Landen, and L. J. Suter, Phys. Plasmas **11**(2), 339 (2004).
- <sup>53</sup>X. T. He and W. Y. Zhang, Eur. Phys. J. D **44**, 227 (2007).